Key comparison BIPM.RI(I)-K2 of the air-kerma standards of the NMIJ and the BIPM in low-energy x-rays

D.T. Burns, A. Nohtomi*, N. Saito*, T. Kurosawa*, N. Takata*

Bureau International des Poids et Mesures, Pavillon de Breteuil, F-92312 Sèvres Cedex
*National Metrology Institute of Japan, AIST, 1-1-1 Umezono, Tsukuba, Ibaraki 305-8568 Japan

Abstract A key comparison has been made between the air-kerma standards of the NMIJ and the BIPM in the low-energy x-ray range. The results show the standards to be in agreement within the expanded uncertainty, although there is evidence of a trend in the results for different radiation qualities. The results are analysed and presented in terms of degrees of equivalence, suitable for entry in the BIPM key comparison database.

1. Introduction

A direct comparison has been made between the air-kerma standards of the National Metrology Institute of Japan (NMIJ) and the Bureau International des Poids et Mesures (BIPM) in the x-ray range from 10 kV to 50 kV. The comparison took place at the BIPM in November 2004 using the reference conditions recommended by the CCRI [1]. Several series of measurements using a transfer ionization chamber were also made at each institute, spanning the period from November 2004 to October 2006.

2. Determination of the air-kerma rate

For a free-air ionization chamber standard with measuring volume V, the air-kerma rate is determined by the relation

$$\dot{K} = \frac{I}{\rho_{\text{air}} V} \frac{W_{\text{air}}}{e} \frac{1}{1-g_{\text{air}}} \prod_i k_i \qquad (1)$$

where ρ_{air} is the density of air under reference conditions, I is the ionization current under the same conditions, W_{air} is the mean energy expended by an electron of charge e to produce an ion pair in air, g_{air} is the fraction of the initial electron energy lost in radiative processes in air, and $\Pi\ k_{\text{i}}$ is the product of the correction factors to be applied to the standard.

The values used for the physical constants ρ_{air} and W_{air}/e are given in Table 1. For use with this dry-air value for ρ_{air}, the ionization current I must be corrected for humidity and for the difference between the density of the air of the measuring volume at the time of measurement and the value given in the table[1].

3. Details of the standards

Both free-air chamber standards are of the conventional parallel-plate design. The measuring volume V is defined by the diameter of the chamber aperture and the length of the collecting region. The BIPM air-kerma standard is described in [2] and the changes made to certain

[1] For an air temperature $T \sim 293$ K, pressure P and relative humidity ~50 % in the measuring volume, this involves a temperature correction T / T_0, a pressure correction P_0 / P, a humidity correction $k_{\text{h}} = 0.9980$, and the factor 1.0002 to account for the compressibility of dry air between $T \sim 293$ K and $T_0 = 273.15$ K.

correction factors in October 2003 are given in [3] and the references therein. Details of the NMIJ standard, which has not previously been compared with the BIPM standard, are given in [4]. The main dimensions, the measuring volume and the polarizing voltage for each standard are shown in Table 2.

Table 1. Physical constants used in the determination of the air-kerma rate

Constant	Value	u_i [a]
ρ_{air} [b]	1.293 0 kg m^{-3}	0.000 1
W_{air} / e	33.97 J C^{-1}	0.001 5

[a] u_i is the relative standard uncertainty.
[b] Density of dry air at T_0 = 273.15 K and P_0 = 101.325 kPa.

Table 2. Main characteristics of the standards

Standard	BIPM	NMIJ
Aperture diameter / mm	9.941	8.012
Air path length / mm	100.0	80.0
Collecting length / mm	15.466	20.26
Electrode separation / mm	70	79.9
Collector width / mm	71	80.44
Measuring volume / mm^3	1 200.4	1 021.4
Polarizing voltage / V	1 500	2 500

3. Comparison procedure

3.1 BIPM irradiation facility and reference beam qualities

The comparison was carried out in the BIPM low-energy x-ray laboratory, which houses a high-voltage generator and a tungsten-anode x-ray tube with an inherent filtration of 1 mm beryllium. A beryllium filter of thickness 2.16 mm is added (for all radiation qualities) so that the half-value layer (HVL) of the present 10 kV radiation quality matches that of the original BIPM x-ray tube when the same aluminium filter is used. The generating potential is stabilized using an additional feedback system of the BIPM. Rather than use a transmission monitor, the anode current is measured and the ionization chamber current normalized for any small deviation from the reference anode current. The resulting variation in the BIPM free-air chamber current over the duration of a comparison is normally not more than 3×10^{-4} in relative value. The radiation qualities used in the range from 10 kV to 50 kV are those recommended by the CCRI [1] and are given in Table 3 in ascending HVL from left to right.

The irradiation area is temperature controlled at around 20 °C and is stable over the duration of a calibration to better than 0.1 °C. Two thermistors, calibrated to a few mK, measure the temperature of the ambient air and the air inside the BIPM standard. Air pressure is measured by means of a calibrated barometer positioned at the height of the beam axis. The relative humidity is controlled within the range 47 % to 53 %.

Table 3. Characteristics of the BIPM reference radiation qualities

Radiation quality	10 kV	30 kV	25 kV	50 kVb	50 kVa
Generating potential / kV	10	30	25	50	50
Additional Al filtration / mm	0	0.208 2	0.372 3	1.008 2	3.989
Al HVL / mm	0.037	0.169	0.242	1.017	2.262
μ_{air} [a] / 10^{-3} mm^{-1}	1.787	0.441	0.314	0.091	0.046
$\dot{K}_{BIPM}$ / mGy s^{-1}	1.00	1.00	1.00	1.00	1.00

[a] Air attenuation coefficient at 293.15 K and 101.325 kPa, measured at the BIPM for an air path length of 100 mm.

3.2 Correction factors

The correction factors applied to the ionization current measured at each radiation quality, together with their associated uncertainties, are given in Table 4 for the BIPM standard and in Table 5 for the NMIJ standard.

Table 4. Correction factors for the BIPM standard

Radiation quality	10 kV	30 kV	25 kV	50 kVb	50 kVa	u_{iA}	u_{iB}
Air attenuation k_a [a]	1.195 7	1.045 1	1.031 9	1.009 1	1.004 6	0.000 2	0.000 1
Scattered radiation k_{sc} [b]	0.9962	0.9972	0.9973	0.9977	0.9979	-	0.000 3
Fluorescence k_{fl} [b]	0.9952	0.9971	0.9969	0.9980	0.9985	-	0.000 5
Electron loss k_e	1.000 0	1.000 0	1.000 0	1.000 0	1.000 0	-	0.000 1
Ion recombination k_s	1.000 6	1.000 7	1.000 7	1.000 7	1.000 7	0.000 1	0.000 1
Polarity k_{pol}	1.000 5	1.000 5	1.000 5	1.000 5	1.000 5	0.000 1	-
Field distortion k_d	1.000 0	1.000 0	1.000 0	1.000 0	1.000 0	-	0.000 7
Aperture edge transmission k_l	1.000 0	1.000 0	1.000 0	1.000 0	1.000 0	-	0.000 1
Wall transmission k_p	1.000 0	1.000 0	1.000 0	1.000 0	1.000 0	0.000 1	-
Humidity k_h	0.998 0	0.998 0	0.998 0	0.998 0	0.998 0	-	0.000 3
$1 - g_{air}$	1.000 0	1.000 0	1.000 0	1.000 0	1.000 0	-	0.000 1

[a] Values for 293.15 K and 101.325 kPa; each measurement is corrected using the air density measured at the time.
[b] Values for k_{sc} and k_{fl} adopted in October 2003, based on Monte Carlo calculations.

The largest correction at low energies is that due to the attenuation of the x-ray fluence along the air path between the reference plane and the centre of the collecting volume. The correction factor k_a is evaluated using the measured air-attenuation coefficients μ_{air} given in Table 3. In practice, the values used for k_a take account of the temperature and pressure of the air in the standard at the time of the measurements. The value for k_a for the NMIJ chamber at 10 kV has

been increased by the factor 1.000 74 to account for the larger mean air-attenuation coefficient for an air path length of 80 mm (the values given in Table 3 were measured at the BIPM for an air path length of 100 mm). This effect is negligible at the other radiation qualities. Ionization measurements are also corrected for changes in air attenuation arising from variations in the temperature and pressure of the ambient air between the radiation source and the reference plane.

Measurements using the BIPM standard were made using positive polarity only. A correction factor of 1.000 5 was applied to correct for the known polarity effect in the standard. Similarly, measurements using the NMIJ standard were made using positive polarity only. A correction factor of 1.000 5 was applied, based on the results of the additional measurements noted in Section 4.3.

All measured ionization currents are corrected for ion recombination. The measured values for the ion recombination correction k_s for the BIPM standard are given in Table 4. For the NMIJ standard, the values for k_s given in Table 5 for the BIPM air-kerma rates are derived from measurements at the NMIJ of the coefficients of initial and volume recombination.

Table 5. Correction factors for the NMIJ standard

Radiation quality	10 kV	30 kV	25 kV	50 kVb	50 kVa	u_{iA}	u_{iB}
Air attenuation k_a[a]	1.154 5	1.035 9	1.025 4	1.007 3	1.003 7	0.000 2	0.000 1
Scattered radiation k_{sc}[b]	0.992 2	0.994 8	0.994 7	0.996 1	0.996 7	-	0.000 8
Electron loss k_e	1.000 0	1.000 0	1.000 0	1.000 0	1.000 0	-	0.000 1
Ion recombination k_s	1.001 0	1.001 0	1.001 0	1.001 0	1.001 0	-	0.000 2
Polarity k_{pol}	1.000 5	1.000 5	1.000 5	1.000 5	1.000 5	0.000 2	-
Field distortion k_d	1.000 0	1.000 0	1.000 0	1.000 0	1.000 0	-	0.000 1
Aperture edge transmission k_l[c]	1.000 0	0.999 8	0.999 8	0.999 3	0.999 0	-	0.000 2
Wall transmission k_p	1.000 0	1.000 0	1.000 0	1.000 0	1.000 0	-	0.000 1
Humidity k_h	0.998	0.998	0.998	0.998	0.998	-	0.000 3
$1 - g_{air}$	1.000 0	1.000 0	1.000 0	1.000 0	1.000 0	-	0.000 1

[a] Values for 293.15 K and 101.325 kPa; each measurement is corrected using the air density measured at the time.
[b] Includes the effect of fluorescence; for the BIPM standard, the separate factor k_{fl} is applied.
[c] Includes the effect of scatter from the aperture.

3.3 Chamber positioning and measurement procedure

The NMIJ chamber was positioned close to the BIPM chamber and both remained fixed throughout the comparison; the alternation of measurements between chambers was carried out by displacement of the radiation source. Alignment on the beam axis was measured to around 0.1 mm and this position was reproducible to better than 0.01 mm. No correction is applied for the radial non-uniformity of the beam; for the given aperture diameters, this effect is estimated to be less than 1×10^{-4} in relative value. The reference plane for each chamber was positioned at 500 mm from the exit window of the x-ray tube, for all qualities. This distance was measured to 0.03 mm and was reproducible to better than 0.01 mm. The beam diameter in the reference plane is 45 mm for all qualities.

The air temperature for the NMIJ chamber was taken to be that of the ambient air. The leakage current was measured before and after each series of ionization current measurements and a correction made based on the mean of these leakage measurements. For the BIPM chamber the leakage current, relative to the ionization current, was less than 1×10^{-4}. For the NMIJ chamber, the relative leakage current under stable conditions was also less than 1×10^{-4}. However, on several occasions during the comparison, immediately after connecting the chamber, the relative leakage current increased to over 5×10^{-3} and decayed to the previous low value over a period of several hours. Fortunately, during such excursions the leakage decayed in a predictable manner and measurements were still possible.

The relative standard uncertainty of the mean of a series of seven measurements for the NMIJ standard was typically below 2×10^{-4}. Repeat measurements for the 25 kV and 50 kVa radiation qualities showed a repeatability not worse than 3×10^{-4} in relative value. Consequently, a type A relative standard uncertainty of 3×10^{-4} is taken for current measurements using the NMIJ chamber. For the BIPM standard, two series of seven current measurements were made (positive polarity only), the mean current for each series being determined with a relative standard uncertainty below 1×10^{-4}.

4. Supporting measurements

4.1 Comparison of methods for measuring air attenuation

The air-attenuation correction for each standard was determined using the air-attenuation coefficients μ_{air} measured at the BIPM, as given in Table 3. These are measured using a tube of length 270 mm positioned approximately midway between the added filters and the reference plane. By reducing the air pressure in the tube to approximately 64 kPa and measuring the decrease in the ionization current, μ_{air} is determined for an air path length of 100 mm. For the 10 kV radiation quality, additional measurements are made over a range of air pressures to determine μ_{air} for other air path lengths, from which the correction factor 1.000 74 for the NMIJ air path length of 80 mm is derived. Note that the thin beryllium windows of the attenuation tube are included in the stated inherent filtration (2.9 mm beryllium).

The NMIJ method for determining μ_{air} is to displace the measuring volume with respect to the fixed aperture by the use of an adapter. A first set of measurements is made under reference conditions, that is, with the aperture at 1 000 mm from the source and with the centre of the measurement volume at 1 080 mm. A second set of measurements employs the adapter to move the chamber body back by 80 mm while keeping the aperture fixed at 1 000 mm. A similar procedure was used at the BIPM. The NMIJ aperture of 6 mm diameter was supported in front of the BIPM standard (with its own aperture removed), fixed with respect to the source, and measurements were made with the chamber body in its reference position, that is, with the measurement volume at 600 mm from the source. A second set of measurements was made with the measurement volume at 700 mm, the difference corresponding to the 100 mm air path length of the BIPM standard. For the calculation of μ_{air}, the air path length was corrected for temperature and pressure, in other words, μ_{air} was evaluated for the reference conditions of 293.15 K and 101.325 kPa.

At 25 kV, the value $\mu_{air} = 0.311\ m^{-1}$ was measured, compared to the BIPM reference value $0.314\ m^{-1}$. The difference corresponds in relative terms to 3×10^{-4} in the air-kerma determination. At 10 kV, the difference was much larger, corresponding to 1×10^{-2} in the air-kerma measurement. However, this is not surprising; the present measurement determines the mean value for μ_{air} with the centre of the measurement volume positioned at 600 mm and 700 mm, whereas the reference BIPM measurement effectively averages between 500 mm and 600 mm. The air attenuation at 10 kV is very sensitive to this difference. Unfortunately, the

BIPM measurement bench does not permit the NMIJ method to be employed at the correct pair of distances. Nevertheless, from previous measurements at 10 kV using the BIPM method at a range of distances, the modified BIPM value $\mu_{air} = 1.689\ m^{-1}$ can be derived for the 600 mm to 700 mm range, compared to the result of the present measurement, $\mu_{air} = 1.690\ m^{-1}$. The difference corresponds in relative terms to only 1×10^{-4} in the air-kerma determination. It is probable that the small difference determined at 25 kV arises from a similar effect.

In conclusion, the NMIJ and BIPM methods are in close agreement. However, to achieve this agreement at 10 kV it is important that the air-attenuation measurement be made at the correct pair of distances. This means that at the NMIJ the measurements should be made with the aperture fixed at 920 mm and with the centre of the measurement volume at 1 000 mm and 1 080 mm (in other words, all components 80 mm closer to the source than at present).

4.2 Comparison of apertures

An adapter was machined to allow the BIPM aperture of diameter 9.941 mm to be positioned in the NMIJ chamber, replacing the NMIJ aperture of diameter 8.012 mm (the converse was not possible because of the large external diameter of the NMIJ aperture). The adapter also displaced the BIPM aperture forward by 3 mm to account for the taper on the inside surface of the NMIJ aperture, thus positioning the reference plane for each aperture at the same distance. The ionization current per unit aperture area was determined for each aperture, the measurements being corrected for ion recombination and aperture edge transmission (k_l in Tables 4 and 5).

The initial results (at 30 kV and 50 kVb) were poor, the BIPM aperture giving a current lower than anticipated by more than 1×10^{-2} in relative value. On close inspection, it was observed that the vertical guard strips behind the aperture are separated by only 10 mm and consequently might attenuate the beam when used with the BIPM aperture. For this reason, subsequent measurements were made using a smaller BIPM aperture, of diameter 4.9992 mm, and the results corrected for the known current ratio for the two BIPM apertures when used in the BIPM standard. These results give much closer agreement. The NMIJ aperture gives a higher value for the current per unit aperture area, the ratio NMIJ / BIPM being 1.000 4, 1.000 4 and 1.000 8 at 10 kV, 30 kV and 50 kVb, respectively (each result with a statistical standard uncertainty of around 2×10^{-4}). It is of note that a relative uncertainty of 8×10^{-4} corresponds to an uncertainty of less than 3 µm in the determination of each aperture diameter. Regarding the variation with radiation quality, this might arise from aperture scatter effects; the NMIJ values for k_l are evaluated by Monte Carlo calculation and include the effect of aperture scatter. Similar calculations are in progress at the BIPM and initial results indicate that scatter and fluorescence from the apertures might be large enough to account for the observed differences.

4.3 Polarity measurements

All comparison measurements were made with the NMIJ standard on positive polarity (2 500 V). In a separate set of measurements, the polarity correction k_{pol} for the NMIJ standard (when used on positive polarity) was measured to be 1.000 57 for the 30 kV radiation quality and 1.000 46 for 50 kVb. Within the statistical uncertainty of 2×10^{-4} these results are not different and the mean value $k_{pol} = 1.000\,5$ was applied to the comparison results for all radiation qualities, as noted in Table 5.

4.4 Calibration of a transfer ionization chamber

As well as the direct comparison of the NMIJ and BIPM free-air chamber standards, a transfer ionization chamber of type PTW 23344, serial number 0889, was calibrated. This chamber had been acquired by the NMIJ just before the comparison in November 2004 and it was not possible to make calibrations at the NMIJ before bringing the chamber to the BIPM. During the

calibration of this chamber at the BIPM, in a radiation field of diameter 45 mm and at the reference distance of 500 mm, it was noted that its relative response changed by about 1.3×10^{-3} over the course of the calibrations. This is not unusual for a new chamber and illustrates why indirect comparisons should not be conducted with a new chamber.

The chamber was subsequently calibrated at the NMIJ in June 2005, also in a field of diameter 45 mm, returned to the BIPM for re-calibration in January 2006, and calibrated again at the NMIJ in March 2006 and in June 2006. Although the chamber response had stabilized at the level of around 1 part in 10^3, there was some doubt over the stability and homogeneity of the small radiation field at the NMIJ and new sets of calibrations were made in the 80 mm diameter field at the NMIJ in September 2006 and again in October 2006. Between this pair of calibrations, the chamber was transported to the BIPM for calibration in the 85 mm field. For all measurements at the NMIJ, the calibration distance was 1000 mm, although this difference in the NMIJ and BIPM calibration arrangements only became evident in March 2007. On noting this, the BIPM calibration coefficients, determined at 500 mm, were corrected to 1000 mm using existing data for this chamber type (the field diameter at 1000 mm is 100 mm). The relative standard uncertainty of this correction is 1×10^3.

The results of the measurements of late 2006 in the large diameter fields are given in Table 6. By comparing the NMIJ results before and after transport to the BIPM, it is evident that the chambers were stable to better than 5 parts in 10^4. As the radiation qualities at the NMIJ and the BIPM are very closely matched, the ratio of the calibration coefficients $N_{K,\mathrm{NMIJ}} / N_{K,\mathrm{BIPM}}$ can be compared directly with the ratio $\dot{K}_{\mathrm{NMIJ}}/\dot{K}_{\mathrm{BIPM}}$ of the air-kerma rate determinations made at the BIPM in November 2004. This comparison of direct and indirect results is discussed in Section 6.

Table 6. Results for the calibration coefficients N_K determined at the NMIJ and at the BIPM in the large diameter radiation fields

	Date	Radiation quality				
PTW 23344-0889		10 kV	30 kV	25 kV	50 kVb	50 kVa
$N_{K,\mathrm{NMIJ}}$ / Gy μC^{-1}	2006-09	88.08	85.86	85.26	83.04	82.67
$N_{K,\mathrm{BIPM}}$[a] / Gy μC^{-1}	2006-09	88.05	85.81	85.15	82.87	82.48
$N_{K,\mathrm{NMIJ}}$ / Gy μC^{-1}	2006-10	88.03	85.88	85.28	83.00	82.69
Ratio $N_{K,\mathrm{NMIJ}} / N_{K,\mathrm{BIPM}}$		**1.0000**	**1.0007**	**1.0014**	**1.0018**	**1.0024**

[a] Calibrations at the BIPM were carried out at the reference distance of 500 mm and corrected to 1000 mm using BIPM data for this chamber type.

5. Uncertainties

The uncertainties associated with the primary standards and with the results of the comparison are listed in Table 7. The uncertainties associated with the measurement of the ionization current and with chamber positioning are those that apply to measurements at the BIPM.

The combined standard uncertainty u_c of the ratio $\dot{K}_{\mathrm{NMIJ}}/\dot{K}_{\mathrm{BIPM}}$ takes into account correlation in the type B uncertainties associated with the determination of the ionization current, the humidity

correction and the physical constants. Correlation in the values for the correction factors k_{sc} and k_{fl} at the BIPM and the factor k_{sc} at the NMIJ, derived from Monte Carlo calculations in each laboratory, are taken into account in an approximate way by assuming half of the uncertainty value for each factor at each laboratory. This is consistent with the analysis of the results of BIPM comparisons in low-energy x-rays in terms of degrees of equivalence described in [11].

Table 7. Uncertainties associated with the comparison results

Standard	BIPM		NMIJ	
Relative standard uncertainty	u_{iA}	u_{iB}	u_{iA}	u_{iB}
Ionization current	0.000 2	0.000 2	0.000 3	0.000 2
Volume	0.000 3	0.000 5	-	0.001 2
Positioning	0.000 1	0.000 1	0.000 1	0.000 1
Correction factors (excl. k_h)	0.000 3	0.000 9	0.000 3	0.000 9
Humidity k_h	-	0.000 3	-	0.000 3
Physical constants	-	0.001 5	-	0.001 5
$\dot{K}_{\text{Standard}}$	0.000 5	0.001 9	0.000 4	0.002 1
	0.001 9		0.002 2	
$\dot{K}_{\text{NMIJ}}/\dot{K}_{\text{BIPM}}$	$u_c = 0.001\,8$ [a]			

[a] Takes account of correlation in Type B uncertainties.

6. Results and discussion

The comparison results are given in Table 8. General agreement at the level of 3×10^{-3} is observed, which is consistent with the expanded uncertainty (with coverage factor $k = 2$) of 3.6×10^{-3}. A trend is observed in the results at different radiation qualities, amounting to around 3×10^{-3}.

The correction factors showing a significant trend with energy are k_a, k_{sc} and k_{fl}. The present results are obtained using air attenuation correction factors measured at the BIPM, for both standards. For this reason, the trend in the comparison results is not likely to arise from the values used for k_a. Regarding k_{sc} and k_{fl}, both laboratories use the Monte Carlo technique for their evaluation. The values used at the BIPM are based on the calculations of Burns [5] using the codes EGSnrc [6] and PENELOPE [7]. Burns [8] also calculated k_{sc} and k_{fl} for a large number of free-air chambers of different dimensions, including an older NMIJ standard. For the present comparison, a new set of calculations was made for the current NMIJ standard (using EGSnrc) and the results are in agreement at the level of around 1 part in 10^3 with those determined by the NMIJ.

Another effect to be considered is that of scatter from the aperture. Calculations by Kurosawa [9] using the MCNP code (version 4B) [10] have shown that scatter from the inner surface of the aperture may increase the measured current for the 50 kVa quality by more than 1 part in 10^3, depending on the aperture diameter, thickness and distance from the source. Conversely, aperture scatter at 10 kV is negligible. A correction for this effect is included in the NMIJ value for k_l in Table 5, although this does not take into account the difference reference distances at the two

laboratories. A Monte Carlo evaluation of aperture scatter for the BIPM standard is in progress, but this is likely to act in the opposite sense to the observed trend with energy. However, there is some indication from these calculations that fluorescence from the tungsten apertures might not be negligible, although the difference between the NMIJ and BIPM apertures is not likely to explain all of the observed trend in the comparison results.

Table 8. Comparison results

Radiation quality	10 kV	30 kV	25 kV	50 kVb	50 kVa
$\dot{K}_{\mathrm{NMIJ}}/\dot{K}_{\mathrm{BIPM}}$	**1.0011**	**1.0006**	**1.0028**	**1.0037**	**1.0045**

Comparing the direct comparison results of Table 8 with those of the indirect comparison given in Table 6 for the PTW chamber, it is evident that there is consistency at the level of around 1×10^3 at the lower radiation qualities, rising to 2×10^3 at the 50 kV qualities. From measurements made using the PTW 23344 chamber type at different field sizes, it is known that field size can have a significant effect on the chamber response and the fact that the NMIJ and BIPM calibration fields are of different diameter might explain the less good agreement between the direct and indirect comparisons at the higher qualities. The results for the indirect comparison should be viewed in the context of the stated relative standard uncertainty for chamber calibration coefficients, which is typically 3.8×10^{-3} for NMIJ calibrations and 2.1×10^{-3} for BIPM calibrations.

7. Degrees of Equivalence

The analysis of the results of BIPM comparisons in low-energy x-rays in terms of degrees of equivalence is described in [11]. Following a decision of the CCRI, the BIPM determination of the air kerma is taken as the key comparison reference value, for each of the CCRI radiation qualities. It follows that for each NMI i having a BIPM comparison result x_i with combined standard uncertainty u_i, the degree of equivalence with respect to the reference value is the difference $D_i = x_i - 1$ and its expanded uncertainty $U_i = 2\,u_i$. The results for D_i and U_i, including those of the present comparison, are shown in Table 9 and in Figure 1, expressed in mGy/Gy as they will be published in the BIPM key comparison database (KCDB).

The degree of equivalence of NMI i with respect to each NMI j is the difference $D_{ij} = D_i - D_j = x_{,i} - x_{,j}$ and its expanded uncertainty $U_{ij} = 2\,u_{ij}$. In evaluating each u_{ij}, correlation between the standards is removed, notably that arising from the physical constants and from k_{e}, k_{sc} and k_{sc}. As described in [11], if correction factors based on Monte Carlo calculations are used by both NMIs, or by neither, then half the uncertainty value is taken for each factor k_{e}, k_{sc} and k_{sc}. Note that the uncertainty of the BIPM determination of air kerma does not enter in u_{ij}, although the uncertainty arising from the comparison procedure is included. The results for D_{ij} and U_{ij} when j represents the NMIJ are also given in Table 9 and in Figure 2. Note that the data presented in the tables, while correct at the time of publication of the present report, will become out-of-date as NMIs make new comparisons. The formal results under the CIPM MRA are those given in the KCDB.

Table 9. Degrees of equivalence. For each NMI i, the degree of equivalence with respect to the key comparison reference value is the difference D_i and its expanded uncertainty U_i, and with respect to NMI j is the difference D_{ij} and its expanded uncertainty U_{ij}. Here j represents the NMIJ. Tables formatted as they appear in the BIPM key comparison database.

10 kV

NMI i	D_i /(mGy/Gy)	U_i /(mGy/Gy)	D_{ij} /(mGy/Gy)	U_{ij} /(mGy/Gy)
NRC	3.7	6.5	2.6	6.8
GUM	-0.7	5.3	-1.8	5.7
NMi-VSL	0.2	4.7	-0.9	5.1
NPL	1.3	4.8	0.2	5.2
NIST	-4.2	5.3	-5.3	5.5
METAS	2.4	3.5	1.3	4.0
ENEA	0.2	5.0	-0.9	5.4
VNIIM	-3.8	5.3	-4.9	5.7
PTB	3.0	5.1	1.9	5.3
BEV	-1.0	4.8	-2.1	5.2
MKEH	1.2	4.1	0.1	4.3
NMIJ	1.1	3.7		

30 kV

NMI i	D_i /(mGy/Gy)	U_i /(mGy/Gy)	D_{ij} /(mGy/Gy)	U_{ij} /(mGy/Gy)
NRC	1.6	6.5	1.0	6.8
GUM	-1.4	5.3	-2.0	5.7
NMi-VSL	-0.3	4.7	-0.9	5.1
NPL	-0.7	4.8	-1.3	5.2
NIST	-5.6	5.3	-6.2	5.5
METAS	0.6	3.5	0.0	4.0
ENEA	-2.9	5.0	-3.5	5.4
VNIIM				
PTB	-3.5	5.1	-4.1	5.3
BEV	-2.8	4.8	-3.4	5.2
MKEH	0.0	4.1	-0.6	4.3
NMIJ	0.6	3.7		

25 kV

NMI i	D_i /(mGy/Gy)	U_i /(mGy/Gy)	D_{ij} /(mGy/Gy)	U_{ij} /(mGy/Gy)
NRC				
GUM				
NMi-VSL				
NPL	1.0	4.8	-1.8	5.2
NIST	-5.3	5.3	-8.1	5.5
METAS	0.9	3.5	-1.9	4.0
ENEA	-2.9	5.0	-5.7	5.4
VNIIM	-3.7	5.3	-6.5	5.7
PTB	-2.2	5.1	-5.0	5.3
BEV	-1.6	4.8	-4.4	5.2
MKEH	0.6	4.1	-2.2	4.3
NMIJ	2.8	3.7		

50 kVb

NMI i	D_i /(mGy/Gy)	U_i /(mGy/Gy)	D_{ij} /(mGy/Gy)	U_{ij} /(mGy/Gy)
NRC				
GUM	-2.3	5.3	-6.0	5.7
NMi-VSL	-0.7	4.7	-4.4	5.1
NPL				
NIST	-6.1	5.3	-9.8	5.5
METAS	-0.7	3.5	-4.4	4.0
ENEA	-2.5	5.0	-6.2	5.4
VNIIM	-2.5	5.3	-6.2	5.7
PTB	-2.2	5.1	-5.9	5.3
BEV	-1.9	4.8	-5.6	5.2
MKEH	0.7	4.1	-3.0	4.3
NMIJ	3.7	3.7		

50 kVa

NMI i	D_i /(mGy/Gy)	U_i /(mGy/Gy)	D_{ij} /(mGy/Gy)	U_{ij} /(mGy/Gy)
NRC	0.2	6.5	-4.3	6.8
GUM	-1.6	5.3	-6.1	5.7
NMi-VSL	-3.0	4.7	-7.5	5.1
NPL	-1.6	4.8	-6.1	5.2
NIST	-4.4	5.3	-8.9	5.5
METAS	-0.8	3.5	-5.3	4.0
ENEA	-2.7	5.0	-7.2	5.4
VNIIM	-1.0	5.3	-5.5	5.7
PTB	-1.1	5.1	-5.6	5.3
BEV	-1.9	4.8	-6.4	5.2
MKEH	0.3	4.1	-4.2	4.3
NMIJ	4.5	3.7		

References

[1] BIPM, Qualités de rayonnement, CCEMRI(I), 1972, R15.

[2] BOUTILLON M., HENRY W.H. and LAMPERTI P.J., Comparison of exposure standards in the 10-50 kV x-ray region, 1969, *Metrologia* **5**, 1-11.

[3] BURNS D.T., Changes to the BIPM primary air-kerma standards for x-rays, 2004, *Metrologia* **41**, L3.

[4] NOHTOMI A., A report on the present status of the low energy x-ray standard at NMIJ, 2004, *AIST Metrology Report* **Vol 2**, **No 4**, 627–632 (in Japanese).

[5] BURNS D.T., New correction factors for the BIPM free-air chamber standards, 2003, CCRI(I)/03-28.

[6] KAWRAKOW I., ROGERS D.W.O., The EGSnrc code system: Monte Carlo simulation of electron and photon transport, 2000, NRCC Report PIRS-701 (National Research Council of Canada).

[7] SALVAT F., FERNANDEZ-VAREA J.M., ACOSTA E., SEMPAU J., PENELOPE - A Code System for Monte Carlo Simulation of Electron and Photon Transport, 2001, Proceedings of a Workshop/Training Course, OECD/NEA, 5-7 November 2001, NEA/NSC/DOC(2001)19 (ISBN 92-64-18475-9).

[8] BURNS D.T., Free-air chamber correction factors for electron loss, photon scatter, fluorescence and bremsstrahlung, 2001, CCRI(I)/01-36.

[9] KUROSAWA T., TAKATA N., Correction factors for free-air ionization chambers for x-rays transmitted through a diaphragm edge and scattered from the surface of the diaphragm aperture, 2005, CCRI(I)/05-27.

[10] BRIESMEISTER J.F., MCNP – A general Monte Carlo N-Particle transport code, version 4B, 1997, *Los Alamos National Laboratory Report* LA-12625-M.

[11] BURNS D.T., Degrees of equivalence for the key comparison BIPM.RI(I)-K2 between national primary standards for low-energy x-rays, 2003, *Metrologia* **40** Technical Supplement, 06031.

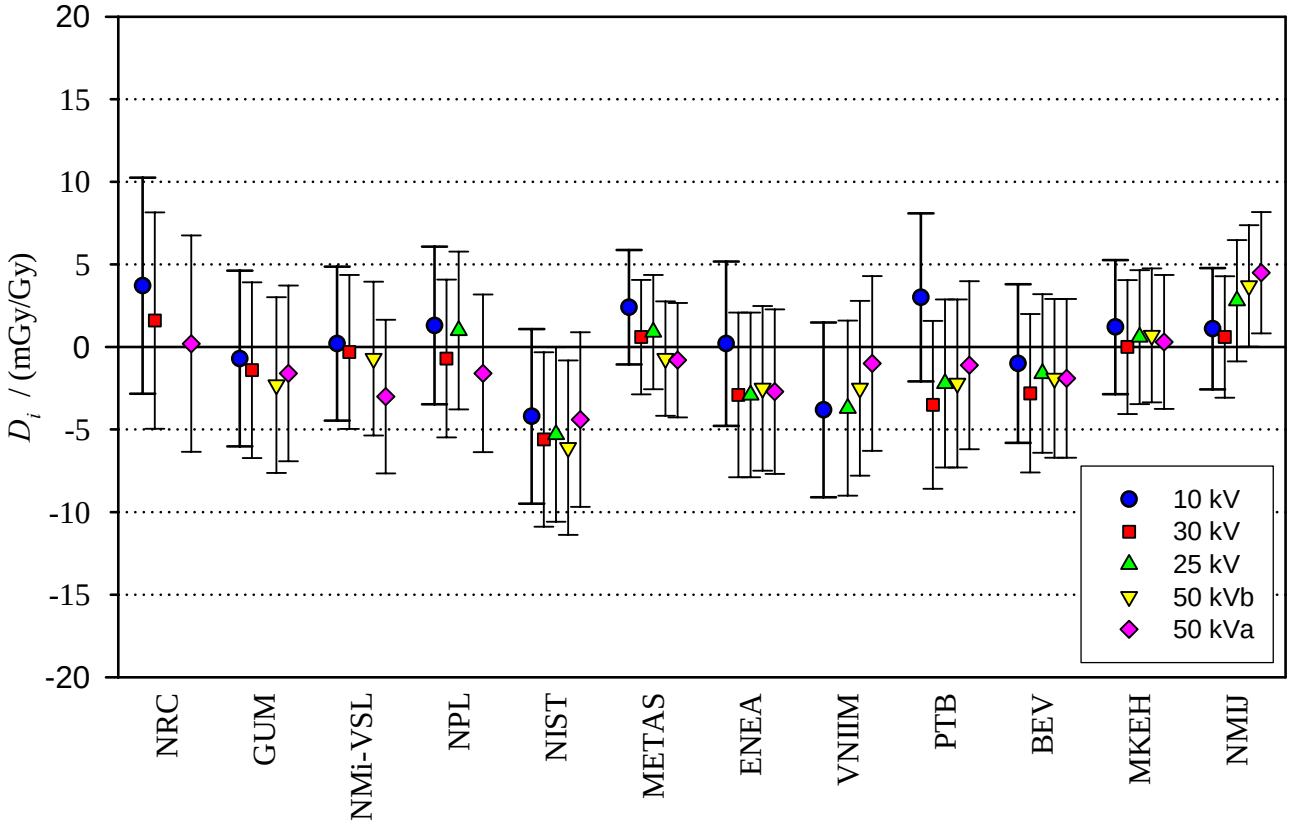

Figure 1. Degrees of equivalence for each NMI *i* with respect to the key comparison reference value

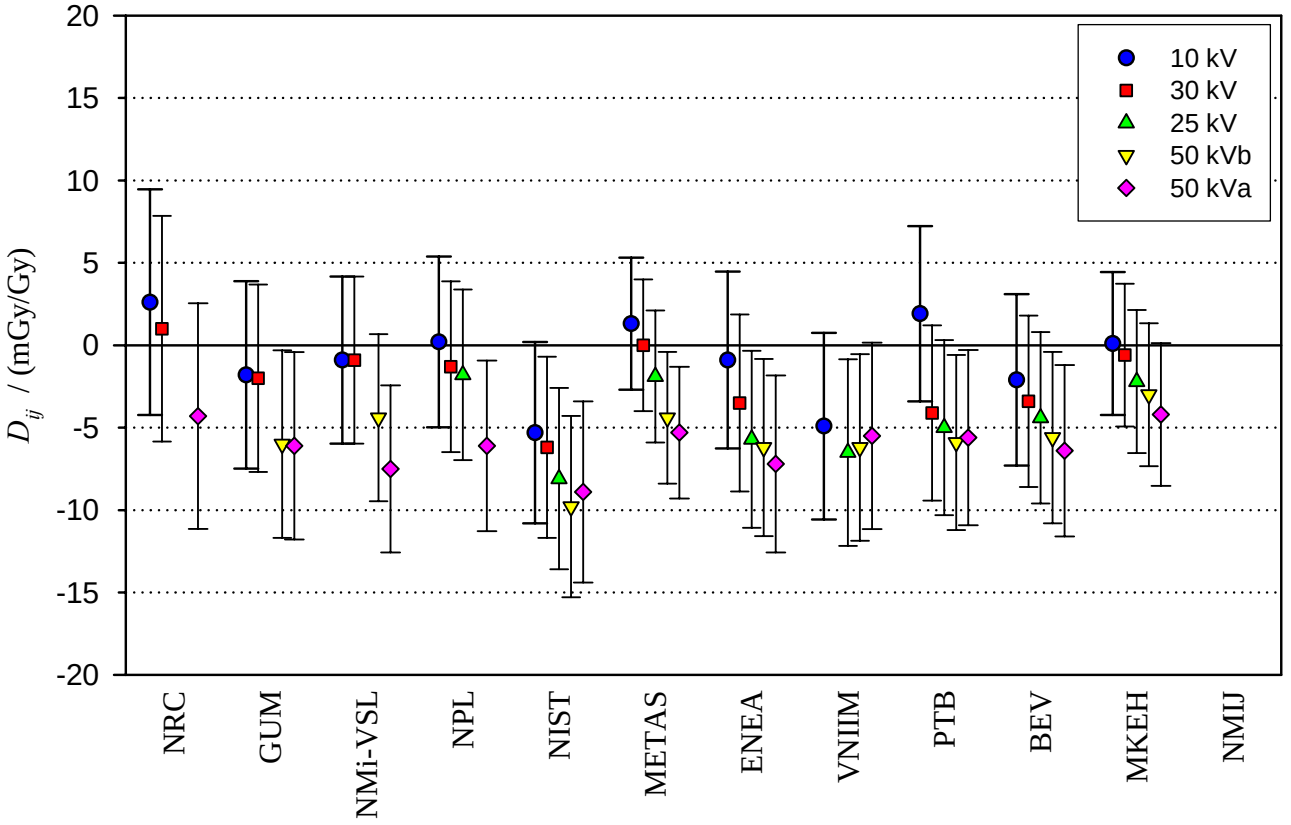

Figure 2. Degrees of equivalence for each NMI *i* with respect to the NMIJ